



Assessment of riverbank erosion and erosion probability using geospatial approach: a case study of the Subansiri River, Assam, India

Kusumbor Bordoloi^{1,2} · Bhaskar Ramachandra Nikam¹ · S. K. Srivastav¹ · Dhrubajyoti Sahariah²

Received: 29 August 2019 / Accepted: 18 December 2019 / Published online: 13 January 2020
© Società Italiana di Fotogrammetria e Topografia (SIFET) 2020

Abstract

Riverbank erosion is one of the key geomorphological problems encountered in the floodplains of the alluvial rivers. Many recent studies on fluvial dynamics have indicated advantages of geospatial technology over traditional techniques in terms of time, cost, and practical usability by the end-users. This study aims to assess the riverbank erosion and erosion probability in a highly dynamic and unstable stretch of the Subansiri River in Assam (India) using geospatial approach along with the Graf's model. Temporal Landsat datasets for a period of 29 years (1989 to 2017) in time step of 4–5 years are used for mapping the river channels (active floodplains) of the Subansiri River. These river channel datasets were then analyzed to spatially quantify the erosion/aggradation and identify the high riverbank erosion zones. Identification and analysis of the high riverbank erosion zones revealed a general westward shift of the Subansiri River during the studied period. The Graf's model, used for estimating the riverbank erosion probability, is implemented in geographical information system (GIS). The transition probability matrices for riverbank erosion were generated for different time spans (1989–1994, 1994–1998, 1998–2002, 2002–2006, 2006–2010, and 2010–2014) using the distance to river channel and erosion/aggradation maps prepared using remote sensing data. Flood recurrence intervals of the annual floods from 1988 to 2017 were estimated using observed discharge data. The transition matrices and flood recurrence intervals were then used to calibrate the Graf's model for estimating the probability of riverbank erosion of the Subansiri River. The results were validated with observed erosion/aggradation map of 2014–2017 time period. The study demonstrates the strength of geospatial approach for rapid assessment of riverbank erosion of alluvial channels. The calibrated Graf's model developed in this study along with understanding of the migration behavior of the Subansiri River will be useful for taking mitigation measures and planning river management strategies.

Keywords Riverbank erosion · Geospatial · Remote sensing · GIS · Graf's model · Subansiri River

Introduction

Rivers are extremely receptive to surrounding environmental settings (Dewan et al. 2017; Eaton et al. 2010; Ety and Rashid 2019; Rozo et al. 2014). The morphological behavior of rivers varies spatially and temporally over different environmental conditions (Akhter et al. 2019; Dewan et al. 2017; Heitmuller

2014; Mount et al. 2013; Sinha and Ghosh 2012). It is the complex outcome of the interactions between the water and sediment transport processes with the factors related to topography, lithology, active tectonics, soil, vegetation cover, land use, and human activities (Akhter et al. 2019; Midha and Mathur 2014; Nanson and Knighton 1996). The spatio-temporal changes in river morphology are more frequent in alluvial rivers (Lanzoni et al. 2018). Riverbank erosion, a geomorphic process, takes place at the time of flood or after the floods in the channels. Through this process, river channels transform their size and shape to transport the upstream contribution of discharge and sediments (Florsheim et al. 2008). Bank erosion accompanied with shifting of river channel is a common hazard, often leading to disasters, for the dwellers living in the vicinity. Due to risk of riverbank erosion, people are forced to relocate from their native lands making them deprived of their basic livelihood. Riverbank

✉ Bhaskar Ramachandra Nikam
bhaskarnikam@iirs.gov.in

¹ Indian Space Research Organisation, Department of Space, Government of India, Indian Institute of Remote Sensing, Indian Institute of Remote Sensing, 4, Kalidas Road, Dehradun, Uttarakhand 248 001, India

² Department of Geography, Gauhati University, Assam, India

erosion not only affects the infrastructure and agriculture but also endangers the riverine ecology of the area (Darby and Thorne 1995; Das et al. 2014).

Channel shifting due to riverbank erosion and its response to the surrounding environmental conditions are predominantly dependent on native elements and hence need local information and locally tuned techniques to model this process (Akhter et al. 2019; Buffington 2012; Khan and Islam 2015). Monitoring riverbank erosion and channel shifting through traditional approaches is time and resource consuming. Satellite remote sensing (owing to its advantage of providing comprehensive and synoptic view of a large area at predetermined temporal interval) and geographical information system (GIS) are valuable tools for monitoring of riverbank erosion and bank line shifting (Sarkar et al. 2012; Thakur et al. 2012; Rozo et al. 2014). Over the last few decades, satellite-based monitoring of riverbank shifting has been widely used for studying the river planform changes and fluvial geomorphological processes. Previous studies have shown that application of satellite remote sensing brings a significant improvement towards quantifying the changes in erosion, river planform, and morphometry (Leys and Werritty 1999; Tiegs and Pohl 2005; Das et al. 2007; Pati et al. 2008; Elliott et al. 2009; Thakur et al. 2012; Lilhare et al. 2014; Nawfee et al. 2018).

Riverbank erosion and channel planform change is a collective phenomenon in riverine ecology. The Subansiri River, the largest north bank tributary (~ 520 km long) of the Brahmaputra River, shows this phenomenon when it enters into Assam State of India from the higher elevations of the Himalayan mountain range. It is a dynamic and unsteady river and distributes its discharge to form an anastomosing arrangement in the river channel and as a consequence meandering courses are formed in the downstream (Singh et al. 2004; Gogoi and Goswami 2013). Riverbank erosion in the Subansiri River in the Assam sector is primarily caused by high water flow and sediment load during the flood period (Gogoi and Goswami 2014). This leads to shifting of the river course with continuous variations in channel morphology and forfeiture of fertile agricultural land and infrastructure in the region (Sarkar et al. 2012; Gogoi and Goswami 2013). Studies related to channel migration and erosion of this river indicate that the river has been shifting its course westward, and after 1920, the river channel has gradually become more extensive due to high sediment deposition on the channel bed (Goswami et al. 1999). After the historic earthquake in 1950, the steadiness between sediment load and transportation of sediment was disrupted because of large-scale landslides in the hilly tracts of the catchment which formed an additional sediment source. After descending into the plains, sediments get deposited in the channels, which leads to channel widening and riverbank erosion (Goswami et al. 1999). The dynamic nature of this river makes the continuous monitoring of riverbank shifting an essential task to ensure safety and sustainability of people living in the vicinity of this river.

Despite availability of many techniques, the identification of erosion susceptible locations and prediction of riverbank erosion is difficult due to dynamic and stochastic nature of the river channels (Winterbottom and Gilvear 2000). Numerical models such as support vector machine (SVM), autoregressive integrated moving average (ARIMA), and artificial neural network (ANN) have been used in fluvial geomorphology to model and predict the riverbank erosion probability (Deb and Ferreira 2015; Sreenu and Teja 2015; Akhter et al. 2019). However, most of these models are not only computationally complex but also data intensive and the detailed datasets required to calibrate and validate these models are generally nonexistent in developing countries. Winterbottom and Gilvear (2000) attempted an integration of relatively less data demanding Graf's model (Graf 1984) in GIS environment to predict the bank erosion probability. Graf's model is based on the spatial location of areas of the floodplain relative to the river channel and flood return interval of the considered time span. It can be easily integrated in GIS environment. Since the model is empirical in nature, it can be calibrated for local conditions with limited observed data making it more suitable for data scarce regions.

The objectives of the present study are twofold: (i) mapping riverbank erosion and identification of high erosion zones using temporal remote sensing data, and (ii) assessment of the riverbank erosion probability by integrating the Graf's model in geospatial environment. The Subansiri River in Assam (India), a dynamic and unstable tributary of the Brahmaputra River, is selected as the study area. Besides understanding the migration behavior of the Subansiri River through spatio-temporal analysis of erosion/aggradation maps, the most significant contribution of this study is the development of calibrated Graf's model for the study area. This calibrated model will be useful for the rapid assessment of riverbank erosion probability of the Subansiri River and planning appropriate mitigation measures by the river management authorities.

Study area and data used

Study area

The Subansiri River is a right-bank tributary of the mighty Brahmaputra River. This is the largest tributary of Brahmaputra River having the length of ~ 520 km and a drainage area of ~ 37,000 km². The word "Subansiri" is taken from the Sanskrit term "*Subarna*" meaning "gold" (Goyal et al. 2018), and the Subansiri River was known as the prospective mining spot for gold in the ancient times. Being the Trans-Himalayan river, the Subansiri is a snow-fed river. The source of this river is located in the western part of mount Pomom (5340 m MSL) in Tibetan Plateau (Goswami et al. 1999).

By meeting three streams in Tibet, namely Tsari Chu, Chayal Chu, and Lokong Chu (Char Chu), the river Subansiri gets formed. Through Miri Hills, Arunachal Pradesh, it arrives in India after flowing through the Himalaya (Goyal et al. 2018). It meets the Brahmaputra at Badati-ghat in the Lakhimpur district of Assam. From its confluence with the Brahmaputra to 100 km upstream is the stretch considered as the study area for the present work (Fig. 1). This is the only stretch of the Subansiri River that runs through a plain area where the problem of riverbank shifting is dominant (Goswami et al. 1999), which justifies the selection of this region for the present study. The entire river stretch which is considered in the present study lies in the Lakhimpur district of Assam. A large number of communities depend on this river for their survival. However, they face many problems like destruction of alluvial agricultural land, loss of human life and live stocks, etc. during and after the flood due to riverbank erosion and sediment deposition.

Geologically, the study area lies in the Quaternary Alluvium (Dikshit and Dikshit 2014). According to the Soil database prepared by the National Bureau of Soil Survey & Landuse Planning (1999), the selected stretch of the river passes through various soil textural classes such as loamy-skeletal, coarse-loamy, coarse-silty, and fine-loamy which

are responsible for slight to very severe erosion. Due to the large expanse from tropical to temperate zones, the Subansiri River basin exhibits a huge variation in rainfall characteristics. The southern part of the river basin receives an ample amount of precipitation due to northeast and southwest monsoon, particularly during May to October, as compared to high altitude region. July and August are identified as the peak flood months of the Subansiri River (Sarkar et al. 2012). Average annual temperature in the river basin also varies considerably, while maximum temperature ranges from 2 to 25 °C and minimum temperature ranges from – 7 to 5 °C (Goyal et al. 2018).

Data used

To achieve the objective of mapping riverbank erosion and identification of high erosion zones in the parts of the Subansiri River, temporal multispectral remote sensing images from Landsat series of satellites are used in the present study. For mapping of river channel and assessment of river planform change, consistent data availability is very essential. Therefore, all the satellite images used in this study with temporal repetivity of 4 to 5 years are of the post-monsoon month (December). Cloud-free standard terrain corrected (L1T) products of optical images from Landsat-5 Thematic Mapper

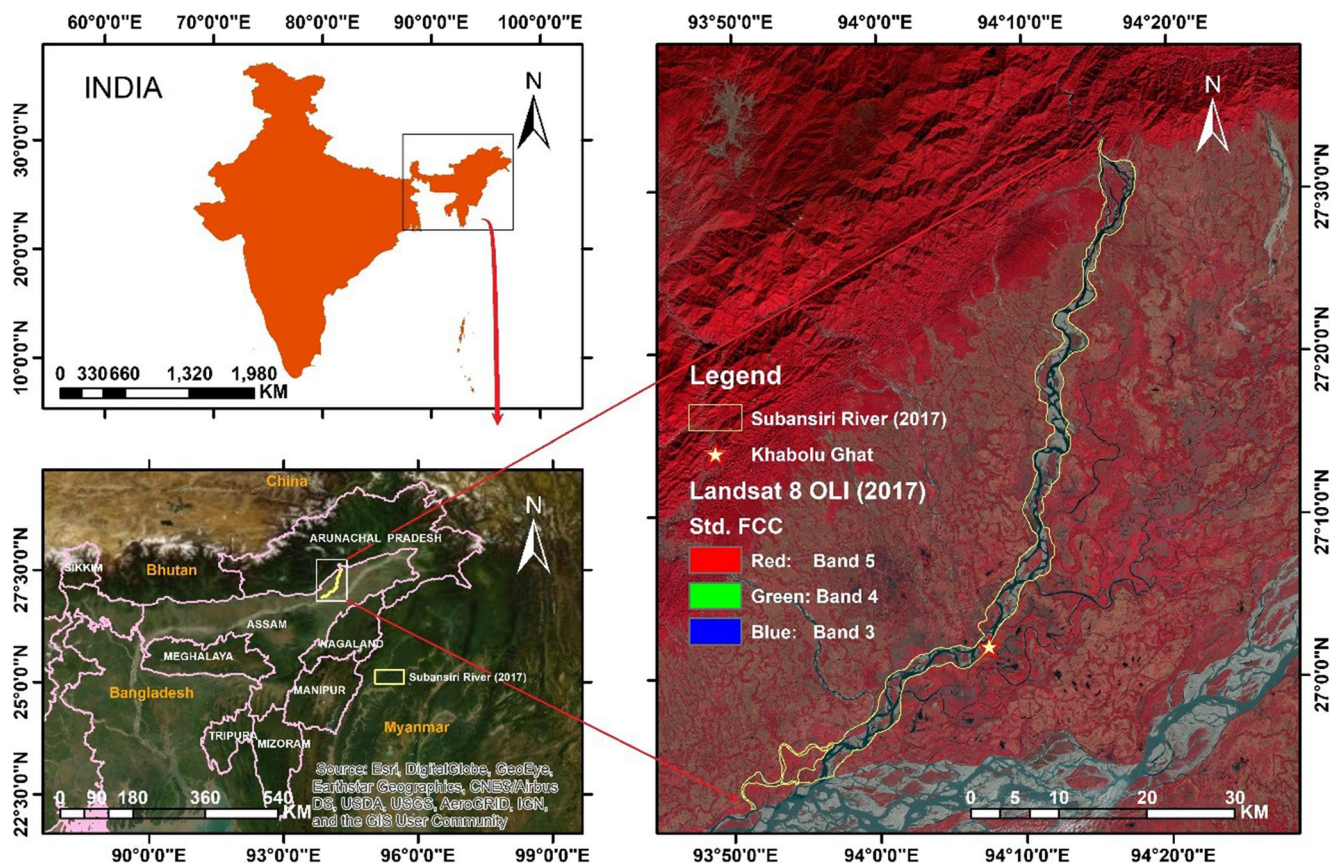


Fig. 1 Location map of the study area: the lower stretch of the Subansiri River in Assam (India) as seen in standard false color composite, derived from Landsat 8 OLI data of 5 December 2017

(TM) and Landsat-8 Operational Land Imager (OLI) for the years 1989, 1994, 1998, 2002, 2006, 2010, 2014, and 2017 are downloaded from the USGS Earth Explorer site (<https://earthexplorer.usgs.gov/>). Table 1 represents all the related information about the satellite imagery used in this study.

To calculate the flood recurrence interval of the Subansiri River, the annual highest flood discharge data of Khabolu Ghat station has been collected from the Water Resource Department, Assam, for the period 1988 to 2017. The station is located at approximately 65 km chainage of the selected stretch, and hence, the flood discharge of this station is considered as average flood inflow of the study area.

Methodology and approach

To achieve the objectives of this study, the efforts were divided into two main domains: (i) mapping river banks and quantification of the riverbank erosion, and (ii) modeling the riverbank erosion by integrating the Graf’s model in the geospatial environment. The overall framework of the methodology used is shown in Fig. 2, and the details are provided in the subsequent subsections.

Quantification of riverbank erosion and identification of high erosion zones

The primary task of the present study was temporal mapping of river channel, quantification of the riverbank erosion with time, and identification of the high erosion zones in the selected stretch of the Subansiri River. As mentioned earlier, temporal multispectral data from Landsat-5 TM and Landsat-8 OLI pertaining to the month of December (post-monsoon) for the period from 1989 to 2017 were acquired and used for this task. Due to low discharge in the river channel in the lean season, a large number of sandbars appear to be scattered within the river channels. Traditionally, researchers have implemented digital image processing techniques for

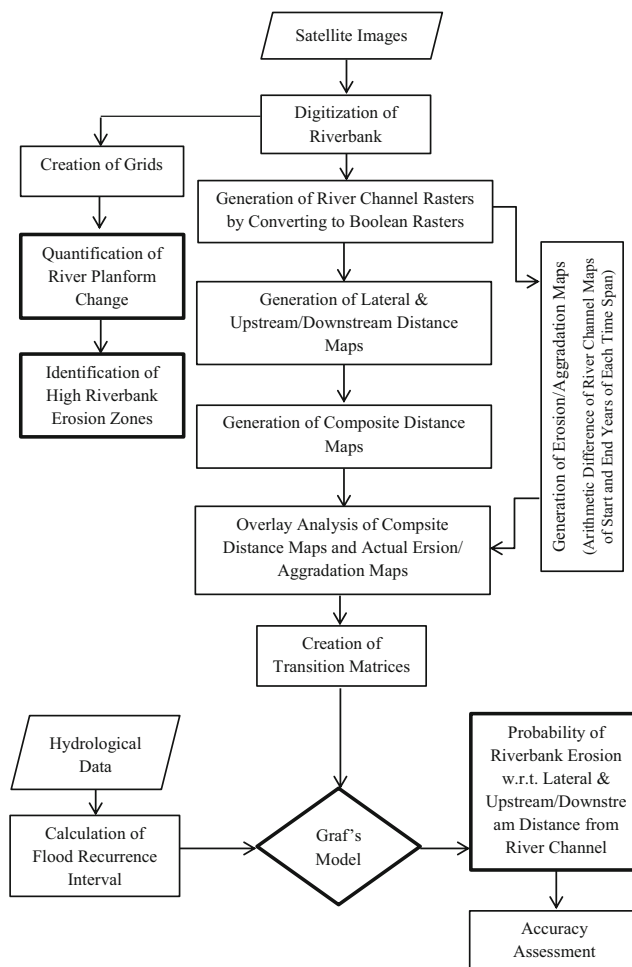


Fig. 2 Methodology framework used in the study

demarcating river channel from other land cover classes; however, presence of channel bars in the river channel and lean season flow in the river make it difficult to accurately map the active floodplain of the river using digital image processing techniques. Considering this, the riverbanks, i.e., active flood plain/river channel (including the channel bars), were digitized manually as a polygon feature in the ArcMap interface

Table 1 Satellite data used in the study

Sl. no.	Data and sensors	Row/ Path	Date of acquisition	Spatial resolution	Cloud cover (%)	Source
1	Landsat 5 TM	41/135	1989-12-08	30 m	7.0	USGS Earth-Explorer (https://earthexplorer.usgs.gov/)
2	Landsat 5 TM	41/135	1994-12-22	30 m	4.0	
3	Landsat 5 TM	41/135	1998-12-17	30 m	4.0	
4	Landsat 5 TM	41/135	2002-12-12	30 m	5.0	
5	Landsat 5 TM	41/135	2006-12-07	30 m	6.0	
6	Landsat 5 TM	41/135	2010-12-18	30 m	7.0	
7	Landsat 8 OLI	41/135	2014-12-29	30 m	3.1	
8	Landsat 8 OLI	41/135	2017-12-05	30 m	5.7	

*All Landsat data used in the study were L1T (standard terrain corrected) products

of ArcGIS (Version 10.5) software using on-screen visual image interpretation technique. The process is repeated for all the temporal images mentioned in Table 1.

For quantifying the erosion and aggradation during each time period, i.e., 1989–1994, 1994–1998, 1998–2002, 2002–2006, 2006–2010, 2010–2014, and 2014–2017, the river channels mapped using remote sensing data were analyzed. For this, the entire study area was divided into square grids of 3 km × 3 km using the “Fishnet” function of ArcGIS. These grids were primarily used for quantifying the erosion/aggradation and for identifying the most critical sections of the river channel in terms of bank erosion. The “symmetrical difference” between the generated square grids and the river channel mapped from each remote sensing image gives the land area and the river channel area in each grid (3 km × 3 km) of the study area. These symmetric difference maps for each year (1989, 1998, 2002, 2006, 2010, 2014, and 2017) were generated and compared with succeeding year’s symmetric difference maps to quantify the erosion and aggradation that has happened during each time period (i.e., 1989–1994, 1994–1998, 1998–2002, 2002–2006, 2006–2010, 2010–2014, and 2014–2017). After quantification of channel planform change, high riverbank erosion zones in each time period were identified based on the calculated value of land area change between two particular years.

Assessment of riverbank erosion probability

An empirical model proposed by Graf (1984) is used in the present study to assess the riverbank erosion probability. According to Graf’s theory, erosion probability of a given cell in a specific duration depends on the position of the cell with respect to the river channel and on the frequency and magnitude of floods coming during that time span. It also states that the position of each cell with respect to the river channel is most significant in the upstream/downstream (i.e., parallel to the river channel) and in the lateral direction (i.e., perpendicular to the river channel) (Fig. 3).

In the Graf’s model, the erosion probability of a particular cell in a given period can be represented as:

$$p_{i,j} = f \left(d_l, d_u, \sum_{t=1}^n r \right) \tag{1}$$

where $p_{i,j}$ represents erosion probability ($0 < p_{i,j} < 1$) of the cell having the coordinates i, j ; f represents the function; d_l represents the lateral distance from the nearby river channel; d_u represents the upstream/downstream distance from the nearby river channel; r depicts the recurrence interval of the highest yearly flood; and n represents the number of years.

In fluvial geomorphic research, distance terms and measures of discharge have been shown to be generally related with erosion by power functions (Leopold et al. 1964), so

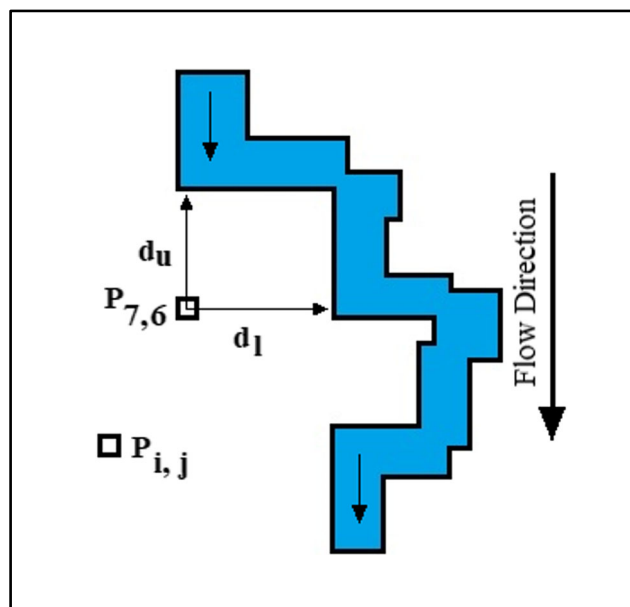


Fig. 3 Schematic diagram of a cell map used in the Graf’s model. Cell $p_{i,j}$ is the arbitrary origin cell; cell $p_{7,6}$ is located seven cells east and six cells north of the origin; channel is represented by shaded cells; d_l is the lateral distance from the cell $p_{7,6}$ to the channel; and d_u is the upstream distance (Graf 1984)

redefined Eq. 1 can be written as:

$$p_{i,j} = a_0(d_l)^{b_1}(d_u)^{b_2} \left(\sum_{t=1}^n r \right)^{b_3} \tag{2}$$

where a_0 and b_1, b_2, b_3 are the constant terms derived empirically based on the past records of riverbank erosion. For $p_{i,j}, d_l, d_u$ and r , mentioned empirical observations in Eq. 2 can be transformed to the linear form as follows:

$$\log_{10} p_{i,j} = \log_{10} a_0 + b_1(\log_{10} d_l) + b_2(\log_{10} d_u) + b_3 \left(\log_{10} \sum_{t=1}^n r \right) \tag{3}$$

The empirically derived constants can then be estimated using *ordinary least squares* technique. Empirical values for the ordered sets of $p_{i,j}, d_l, d_u, \sum_{t=1}^n r$ can be determined from transition matrices (Graf 1984; Winterbottom and Gilvear 2000).

From the transition matrices, erosion probability for each distance class can be calculated using the following formula:

$$p_{i,j} = \frac{C_e}{C} \tag{4}$$

where C_e is eroded cells of a particular distance class in a specific period; C is the number of cells in the distance class.

As discussed in the previous paragraph, the lateral distance and upstream/downstream distance of any point from the river channel are the important inputs for estimating the probability

of that point getting eroded. The stepwise procedure followed in the present study for generating these distance maps for all the years under consideration and estimation of elements of transition matrices is given below:

- 1) *Rasterization of digitized river channels*: As discussed in the “Quantification of riverbank erosion and identification of high erosion zones” section, the river channel of the Subansiri River for years 1989, 1994, 1998, 2002, 2006, 2010, 2014, and 2017 were mapped using visual interpretation and on-screen digitization techniques. Since the Graf’s model is suitable for application on raster datasets, the mapped river channel and its surrounding area is converted in the Boolean rasters of 100 m pixel size (spatial resolution). Value 1 is assigned to the pixels representing river channels and value 0 is given to all other land cover classes. These Boolean rasters are then used for generation of distance (lateral and upstream/downstream) rasters of respective years and generation of erosion/aggradation raster for each time step (e.g., 1989–1994, 1994–1998, 1998–2002, 2002–2006, 2006–2010, 2014–2014, and 2004–2017).
- 2) *Generation of distance raster*: The river channel maps (raster) generated for each year under consideration were used for the generation of lateral and upstream/downstream distance rasters for each year. Calculation of lateral and upstream/downstream distance of the pixels under other land cover classes (e.g., pixels having value 0 in river channel raster) from the river channel was done using the “User-defined Kernel Filter” tool available in Idrisi image processing software. The “User-defined Kernel Filter” estimates distance in either longitudinal (lateral, d_l) or latitudinal (upstream/downstream, d_u) direction of each pivot pixel from the nearest pixels of defined class (river channel). Using this filter function, lateral distance (Fig. 7) and upstream/downstream distance (Fig. 8) maps were generated for all the years under consideration. For simplicity of operations and better representation, the lateral distance and upstream/downstream distance maps were classified into 4 (lateral) and 5 (upstream/downstream) classes, i.e., 100 m, 200 m, 300 m, 400–800 m, and > 800 m distance from river channel, as shown in Figs. 7 and 8, respectively. To reduce the number of raster layers taking part in solving Eq. 3, a composite distance raster of each year was generated by crossing/merging lateral and upstream/downstream distance rasters of respective years. The crossing/merging of two classified raster layers with 5 discrete classes in each layer yielded 21 valid combinations (Table 2) of lateral and upstream/downstream distance classes, which were considered for generation of transition matrix of riverbank erosion. Classified merged/crossed distance

Table 2 Classification of distance classes

d_l	d_u	Class	d_l	d_u	Class
> 800	800+	0	–	–	–
100	100	1	300	100	11
100	200	2	300	200	12
100	300	3	300	300	13
100	400–800	4	300	400–800	14
100	800+	5	300	800+	15
200	100	6	400–800	100	16
200	200	7	400–800	200	17
200	300	8	400–800	300	18
200	400–800	9	400–800	400–800	19
200	800+	10	400–800	800+	20

rasters are termed as composite distance raster (Fig. 9) henceforth.

- 3) *Estimation of transition matrix for each time step*: The raster maps of actual erosion and aggradation area during a time step under consideration, i.e., 1989–1994, 1994–1998, 1998–2002, 2002–2006, 2006–2010, 2010–2014, and 2014–2017 were generated by taking arithmetic difference of river channel rasters of start year and end year of the time step under consideration. Figure 10 indicates erosion/aggradation raster generated for the time step 1989–1994. The red color indicates the area lost due to riverbank erosion and green color indicates area gained or where aggradation has occurred. The composite distance maps of the start year of each time step (e.g., year 1989, Fig. 9 in this case) and the erosion/aggradation maps of the time step under consideration (1989–1994 in present case) are used to generate transition matrix of the considered time step. The total number of pixels (C) under a specific composite (merged) distance class were estimated from composite distance raster. Number of pixels that were eroded (C_e) during the time step out of each composite (merged) distance class are estimated by crossing/merging the composite distance and erosion/aggradation rasters of specific time step (e.g., Figs. 9 and 10). The transition probability of each composite distance class was calculated using this information (C and C_e). The transition matrices for all the time periods (1989–1994, 1994–1998, 1998–2002, 2002–2006, 2006–2010, 2010–2014, and 2014–2017) were estimated using this methodology.

In the Graf’s model, along with distance class and its transition probability, the flood recurrence interval is one of the essential inputs. Recurrence interval or flood frequency analysis is a statistical method by which prediction of flood flow as well as other hydrological processes may be done using

hydrological data series (i.e., annual series constituting yearly maximum flood data from a particular catchment area for a large number of consecutive years). By arranging the data in decreasing order of magnitude (plotting position technique), probability of exceedance (P) is estimated by Weibull formula (Subramanya 2008):

$$P = \frac{m}{N + 1} \tag{5}$$

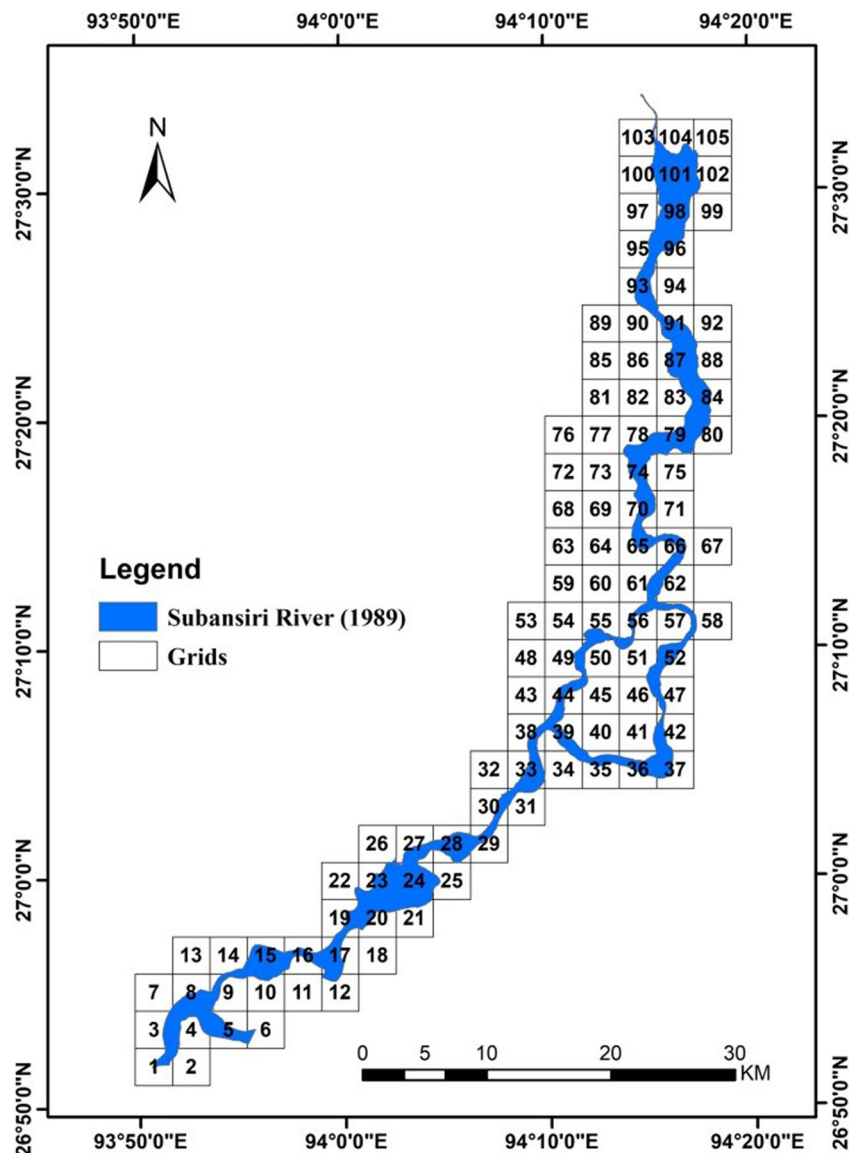
where m represents the order number of the event and N represents the summation of events within the data. Therefore, the recurrence interval, r , is calculated as:

$$r = \frac{1}{P} = \frac{N + 1}{m} \tag{6}$$

In the present study, the annual peak discharge (flood discharge) data of the Subansiri River observed at Khabolu Ghat station for 30 years (1988–2017) were analyzed to estimate flood recurrence interval by arranging the flood discharge data into descending order with respect to the magnitude of discharge and using Eq. 6.

The transition matrices and flood recurrence interval values for 1989–2014 period were used to estimate the empirically derived constants of Eq. 3 by solving it using *ordinary least squares* technique. It is important to note that the transition matrix and flood recurrence interval of 2014 to 2017 period were not utilized in deriving the empirical constants of the Graf’s model. The applicability of empirically derived constants of the Graf’s model was validated by applying the model on the datasets of time period 2014–2017. The model was implemented using composite distance map of 2014 and the summation of recurrence interval of annual floods occurred in

Fig. 4 Overlay of square grids and river channel mapped in December 1989



this duration. The riverbank erosion probability map for the end of period (i.e., 2017) was generated using the Graf's model. The erosion probability map was compared with the actual erosion map, derived from 2014 and 2017 river channel maps, to validate the results obtained through geospatial modeling.

Results and discussion

Quantification of the riverbank erosion

The river channel of the Subansiri River for the years 1989, 1994, 1998, 2002, 2006, 2010, 2014, and 2017 were mapped using temporal remote sensing images obtained from Landsat series of satellites. The study area was divided into the square grids of $3 \text{ km} \times 3 \text{ km}$. The river channel maps were overlaid on grid map (Fig. 4) and the “symmetric difference” between grids and active river channel for each year was taken to estimate the river channel and other land cover class in each grid. The comparison of symmetric difference maps of each year with the successive years gives the erosion or aggradation area in that duration.

The changes in the area (erosion/aggradation) during 1989–1994, 1994–1998, 1998–2002, 2002–2006, 2006–2010, 2010–2014, and 2014–2017 in each grid along the river channel of the Subansiri River are analyzed and are represented in Fig. 5. It is observed that during 1989–1994, grid nos. 23 and 62 show the highest erosion (Fig. 5a), wherein about 2.25 km^2 and 2.26 km^2 land was eroded, respectively, in both the grids. During this period, a total of 37.73 km^2 land got eroded due to riverbank erosion and the aggradation has happened over 11.86 km^2 area. Similarly, during 1994–1998, the highest erosion (2.36 km^2) is recorded in grid no. 85 (Fig. 5b), while a total of 20.20 km^2 area got eroded and the aggradation happened over 36.69 km^2 area. Grid nos. 11 and 69 have suffered maximum erosion, 4.07 km^2 and 3.88 km^2 , respectively during 1998–2002 (Fig. 5c). Overall, 51.17 km^2 of land got eroded and aggradation happened over 69.03 km^2 of land within this time span. Similarly, during 2002–2006, grid nos. 73 and 77 recorded the maximum erosion (Fig. 5d) of 1.65 km^2 and 1.38 km^2 area, respectively. In this period, the total area affected by erosion and aggradation is around 16.18 km^2 and 9.37 km^2 , respectively. During the years 2006–2010, grid no. 64 has shown the highest erosion where 1.32 km^2 land area got eroded (Fig. 5e) and total riverbank

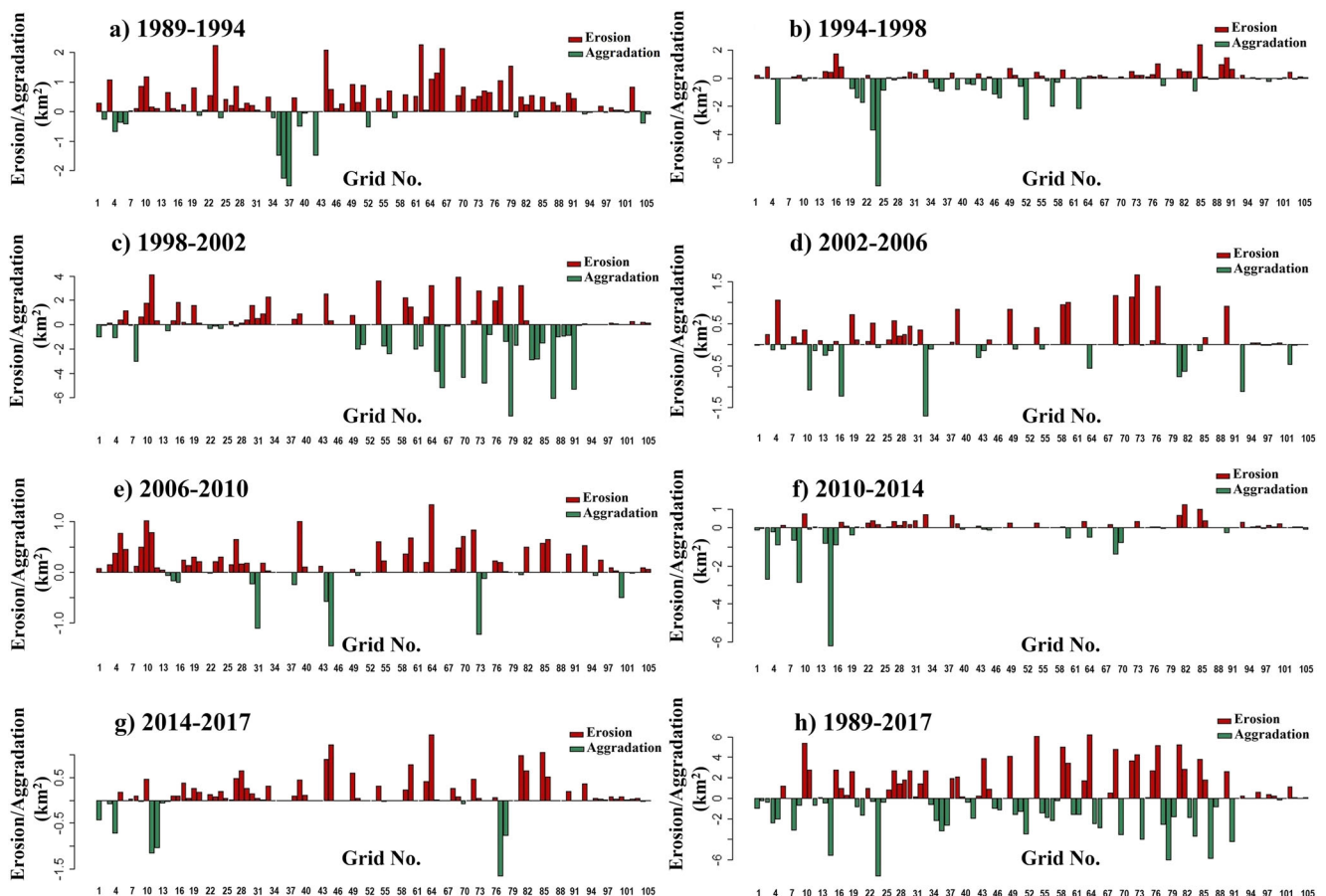


Fig. 5 Grid-wise erosion/aggradation areas in different time spans

erosion of 17.18 km² and aggradation of 6.18 km² have occurred. In 2010–2014, grid no. 82 and 85 recorded erosion of 1.21 km² and 1 km² (Fig. 5f) with total eroded and deposited area of 11.09 km² and 19.15 km², respectively. In recent times, i.e. 2014–2017, it is observed that grid no. 64 and 45 recorded maximum erosion (Fig. 5g) with a loss of 1.43 km² and 1.22 km² land area. The total eroded area in this period is 15.15 km², whereas the total area gained due to aggradation is around 11.38 km².

The comparison between symmetric difference maps of 1989 and 2017 depicts that during the this period, grid nos. 54 and 64 show the maximum erosion, i.e., 6.07 km² and 6.16 km², respectively (Fig. 5h). During this time span, total of 102.63 km² land area got eroded, while aggradation (gained land) occurred over 97.59 km² area. The quantification of the riverbank erosion reveals that the amount of erosion has been fluctuating spatially and temporally in the study area and eroded area is comparatively higher with respect to the area gained due to the shifting of river course. Though the comparison of riverbank erosion of one alluvial river with the bank erosion of another river may not yield a significant conclusion, however, it may

validate the overall shifting behavior of alluvial rivers. Thakur et al. (2012) reported loss of around 16.7 km² area to riverbank erosion between 1955 and 2005 in the study region of 525.56 km² along the Ganga River upstream of Farakka barrage in Manikchak and Kaliachak-II blocks of Malda, West Bengal (India). Similarly, Dewan et al. (2017) reported that both the banks of the Padma River in Bangladesh experienced considerable loss of land of around 155 km² and 28 km² on left and right banks, respectively over the period 1973 to 2011. Nawfee et al. (2018) also reported loss of around 281 km² land area to riverbank erosion from 1973 to 2014 in the selected reaches of Padma River in Bangladesh. All these published results indicate high variability in the rate of riverbank erosion in the alluvial region and that the behavior of the Subansiri River is similar to other rivers.

Identification of high erosion zones

Identification of the high riverbank erosion zones depending on the rate of erosion and aggradation is one of the most needed analysis in the alluvial flood plains. The

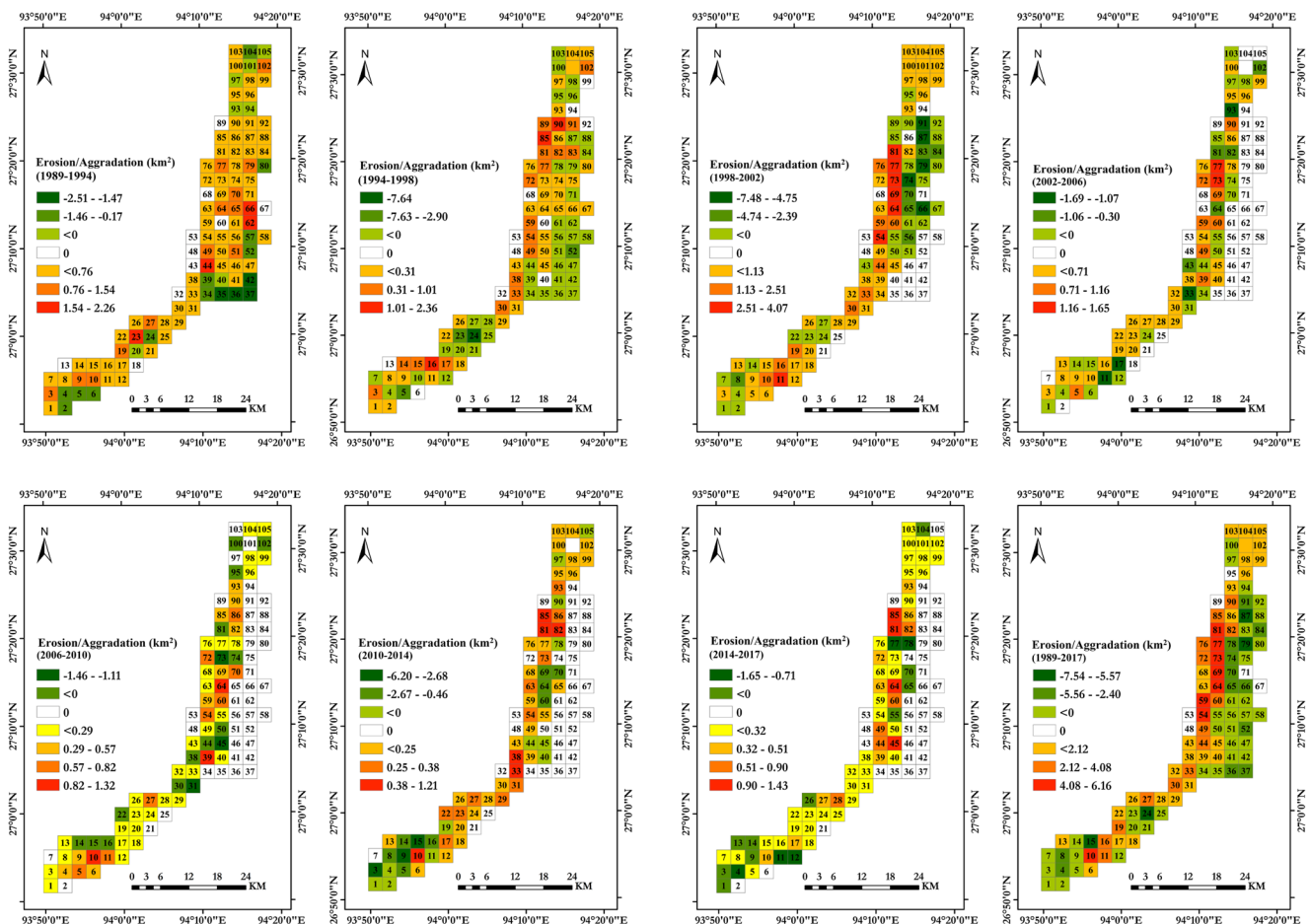


Fig. 6 Grid-wise erosion/aggradation zones in different time steps. Red color represents erosion, while green color represents aggradation. Numbers inside the grid are the unique numbers assigned to each grid

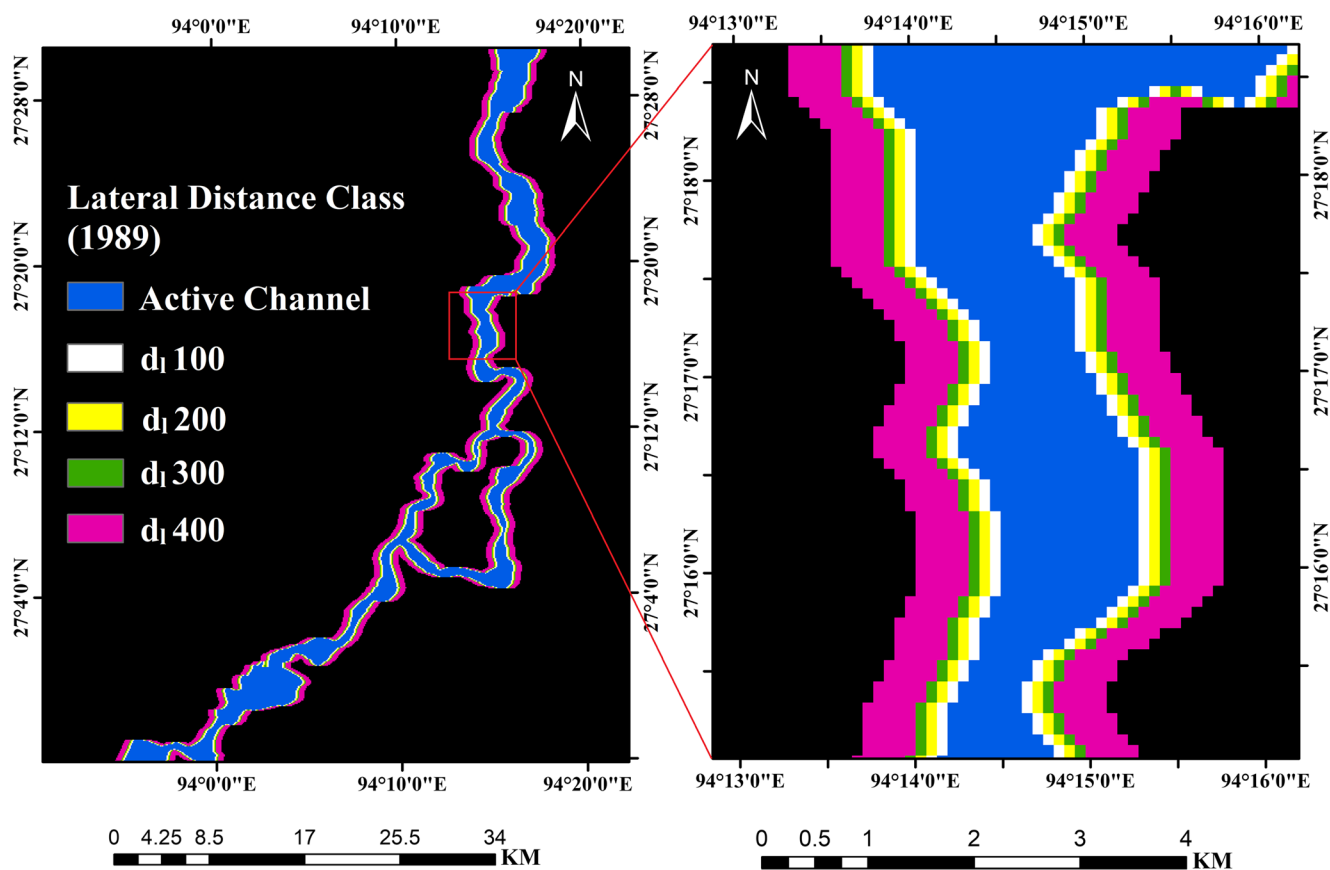


Fig. 7 Map of lateral distance classes for the year 1989

erosion and aggradation values obtained from the analysis described in the previous section were used to generate the erosion/aggradation maps. Figure 6 shows the grid-wise (3 km × 3 km) erosion/aggradation in each time step. Dark red grids depict the highest erosion zones, while dark green represents the high negative erosion, i.e. aggradation zones. White color portrays the stable/unaffected zones where neither erosion nor aggradation has taken place due to shifting of river course.

From Fig. 6, it is observed that during 1989–1994, grid no. 23, 44, 62, 66 have undergone high riverbank erosion (1.54 to 2.26 km²). On the other hand, grid no. 35, 36, 37, 42 show maximum aggradation (1.47 to 2.51 km²) during the same time period. Similarly, during 1994–1998, grid no. 16, 85, 90 are indicated as high erosion zones (1.01 to 2.36 km²) and maximum aggradation has taken place in the grid no. 24 (7.64 km²). From 1998 to 2002, identified high erosion zones include grid nos. 54, 64, 69, 73, 77, and 81 (2.51 to 4.07 km²). During the same period, maximum aggradation is recorded in grid nos. 66, 74, 79, 87, and 91 (4.75 to 7.48 km²). During 2002–2006, grid nos. 73 and 77 have experienced high erosion (1.16 to 1.65 km²) and grid nos. 11, 17, 33, and 93 show higher aggradation (1.07 to 1.69 km²). During 2006–2010, identified high erosion zones were at grid nos. 10, 39, and 64 (1.16 to 1.65 km²). During the time span of 2010–2014,

grid nos. 10, 33, 38, 81, 82, and 85 are under high erosion (0.38 to 1.21 km²). Grid no. 45, 81, and 85 show high erosion during 2014–2017 (0.90 to 1.43 km²), whereas maximum aggradation occurred in grid nos. 4, 11, 12, 77, and 78 (0.71 to 1.65 km²). The comparison between year 1989 and 2017 revealed that grid nos. 54, 59, 64, 69, 73, 77, and 81 are the zones with maximum erosion (4.08 to 6.16 km²). It is also evident from Fig. 6 that the grids on the eastern side of the river channel have gradually migrated into no erosion or aggradation zone with the progress of time. At the same time, the grids on the western side of the river channel show an increase in erosion with time. This temporal analysis of high erosion/aggradation zones (Fig. 6) indicates the shifting of the Subansiri River towards the western side. Such westward shifting of the Subansiri River was also observed and highlighted by Goswami et al. (1999). According to them, the Subansiri River shifted 6 km westward in upstream reaches near Chauldhoaghat during 1920–1970. On the other hand, unequal shifting of both bank lines in both directions increased the channel width during 1970–1990. Based on the study of 184 years (from 1828 to 2011), Gogoi and Goswami (2014) have also shown that the Subansiri has consistently laterally migrated towards the west. Therefore, the direction of shift observed in the present study matches with the published literature. Quantification of spatial erosion/aggradation

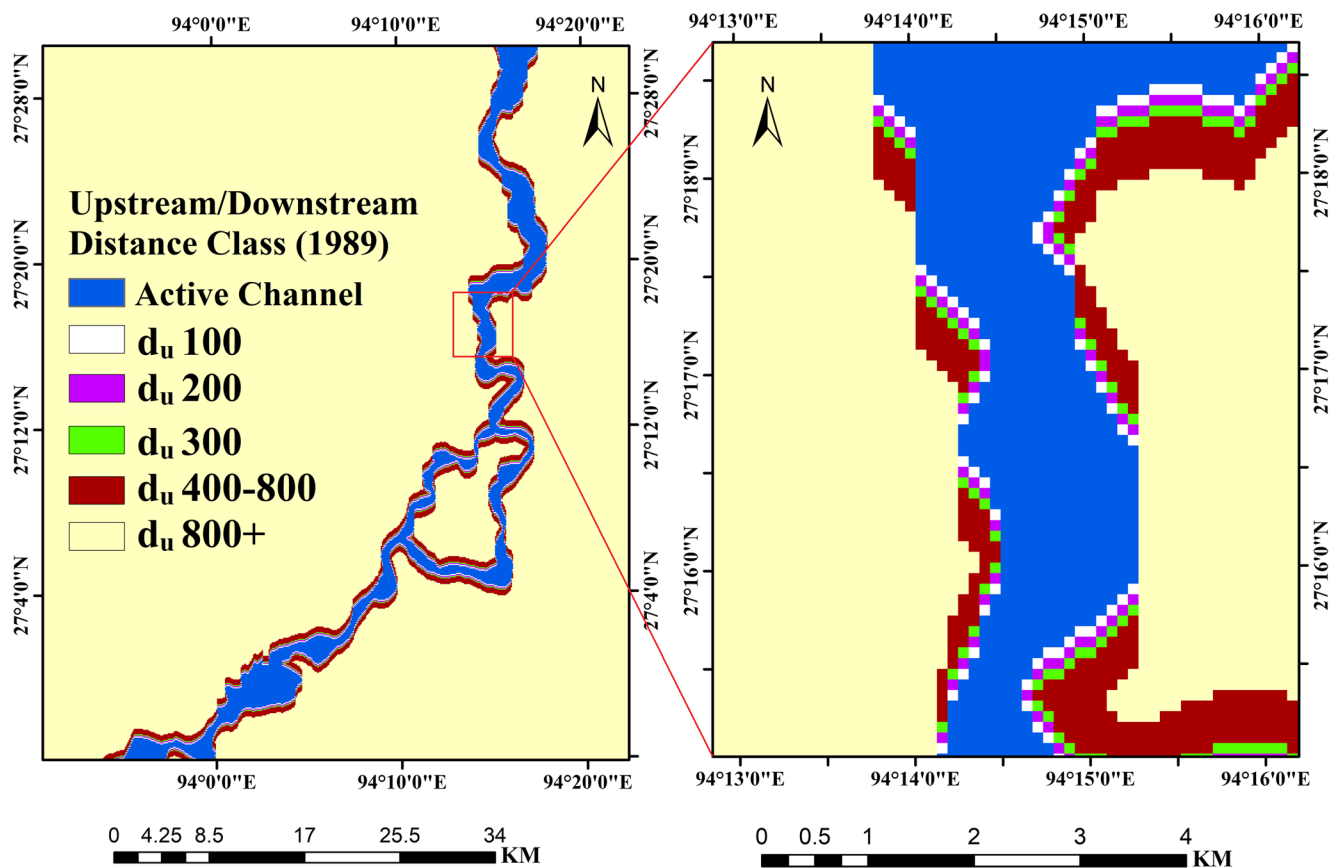


Fig. 8 Upstream/downstream distance classes for the year 1989

carried out in this study further aids to comprehend the rate of change as well as the dynamic behaviour of the river.

Assessment of riverbank erosion probability using Graf's model

The input datasets preparation for the implementation of Graf's model was done through various steps as described in the "Methodology and approach" section. The results of input preparation and model application are described here.

Lateral and upstream/downstream distance classes

The river channel maps, derived through digitizing active floodplains for each specified year, were converted into Boolean rasters of 100 m pixel size. These Boolean rasters were utilized for the generation of lateral and upstream/downstream distance maps from river channels. For ease in analysis, in the present study, the lateral distance rasters/maps were classified into four (04) discrete categories (100 m, 200 m, 300 m, and 400–800 m) and the classes are denoted as dl100, dl200, dl300, and dl400–800, respectively (Fig. 7). The upstream/downstream distance rasters/maps of all the years were classified into five different distance classes

(100 m, 200 m, 300 m, 400–800 m, and < 800 m) and denoted by du100, du200, du300, du400–800, and du800+ (Fig. 8).

For each year of analysis, the composites distance maps were generated by merging/crossing the lateral and upstream/downstream distance maps of respective year (1989, 1994, 1998, 2002, 2006, 2010, 2014, and 2017). New class identifier is assigned to the merged classes. Total 21 different combinations of distance classes are considered in the present study. Table 2 describes assigned class numbers according to their combination of distance classes. Figure 9 shows the composite distance class map for the year 1989. Similar maps for all the years under consideration were also prepared.

Formation of transition matrices

The river channel rasters were used for mapping and quantifying the erosion and aggradation areas in each time step. The algebraic difference between the river channel rasters of start and end years of the time step (e.g., for period 1989–1994, river channel raster of 1989 minus river channel raster of 1994) gives the erosion and aggradation area in that period. Figure 10 shows the erosion/aggradation area map derived from 1989 to 1994 river channel rasters. In this figure, areas with red color depict the eroded pixels and the green areas represent aggraded pixels. During this time span, 3961 land

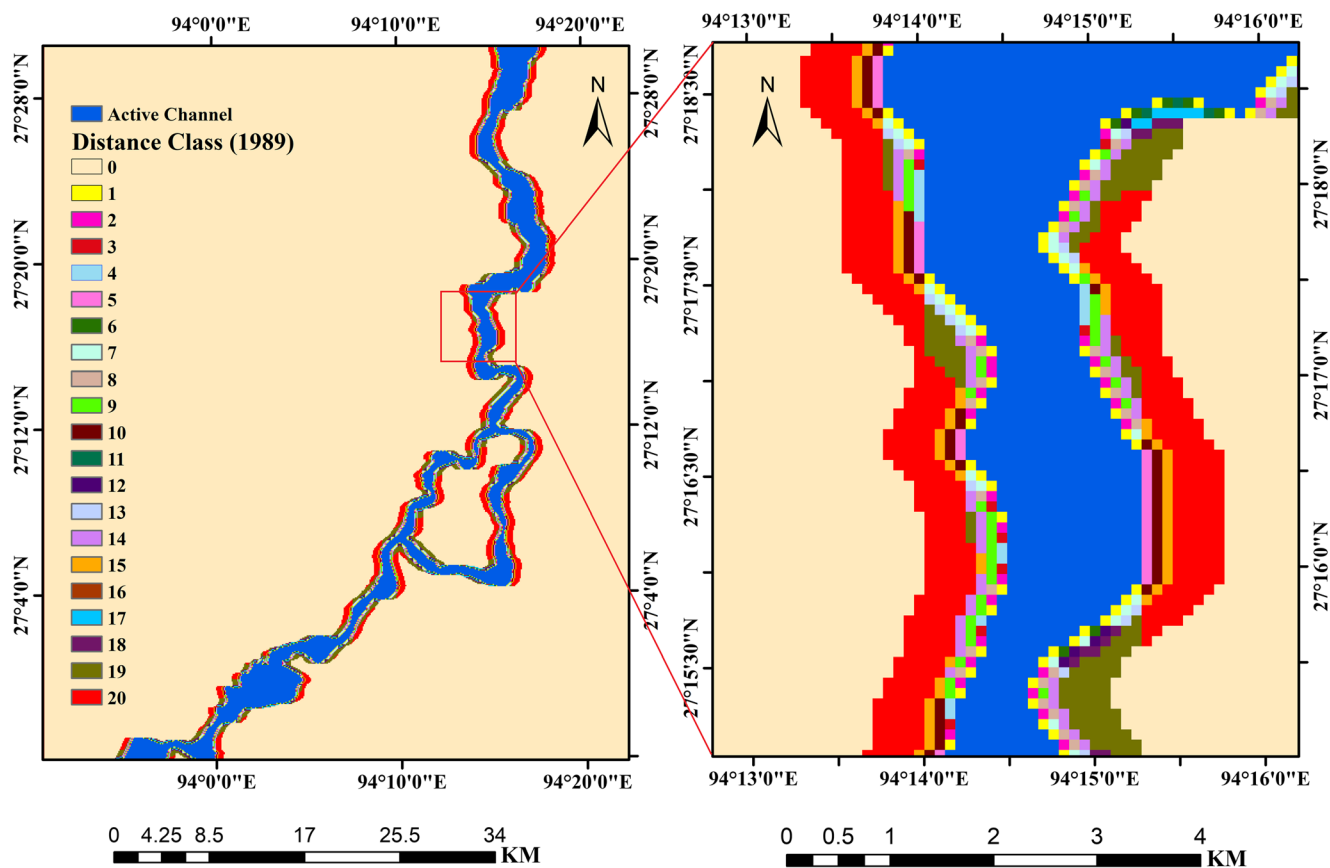


Fig. 9 Map of composite distance classes for the year 1989

pixels were eroded and aggradation has occurred in 1387 pixels. Similarly, the erosion/aggradation areas for each time step were estimated using the river channel rasters of respective years.

To generate the transition probability matrices for different time steps, an overlay analysis between composite distance rasters of start year, i.e., classified distance map of start year (e.g., Fig. 9) and the erosion/aggradation maps (Fig. 10) of the respective time step was performed. In the overlay analysis, using the “Raster Calculator” in ArcGIS, number of land pixels that are eroded and number of pixels that are not eroded during the time period under consideration were estimated for each composite distance class (Table 3). In Table 3, C represents the total number of pixels that belong to a specific distance class in the given time, C_e depicts the number of pixels that are eroded within the time span under consideration and $P_{i,j}$ represents the probability of erosion. Using similar methodology, the transition matrices for all the time steps (e.g., 1989–1994, 1994–1998, 1998–2002, 2002–2006, 2006–2010, and 2010–2014) were generated.

Flood recurrence interval

The return periods (r) of all the annual flood events, from 1988 to 2017, observed in the Subansiri River were calculated using

probability analysis (Table 4). Due to the restriction on publishing the river discharge data, the actual flood flow values are not given in Table 4, however, the return period of each annual flood is indicated in the table. Further, the flood recurrence intervals ($\sum_{i=1}^n r$) for all the specific time spans, i.e., 1989–1994, 1994–1998, 1998–2002, 2002–2006, 2006–2010, and 2010–2014 were calculated (Table 5).

Prediction of erosion probability using Graf’s model

From the transition matrices of each time period (1989–1994, 1994–1998, 1998–2002, 2002–2006, 2006–2010, and 2010–2014), total 127 sets of $p_{i,j}$, d_l , d_u and $\sum_{i=1}^n r$ were available for solving Eq. 3 by using the *ordinary least squares* technique. The multi-parameter regression solution of Eq. 3 resulted in the coefficient of determination (R^2) value of 0.63 and the value of the empirical coefficients, i.e., a_0 and b_1, b_2, b_3 is estimated as 1360.21, -0.996 , -0.669 , and 0.263, respectively. Therefore, Eq. 2 for our study area (i.e., trained Graf’s model) can be written as:

$$P_{i,j} = 1360.21(d_l)^{-0.996}(d_u)^{-0.669}\left(\sum_{t=1}^n r\right)^{0.263} \tag{7}$$

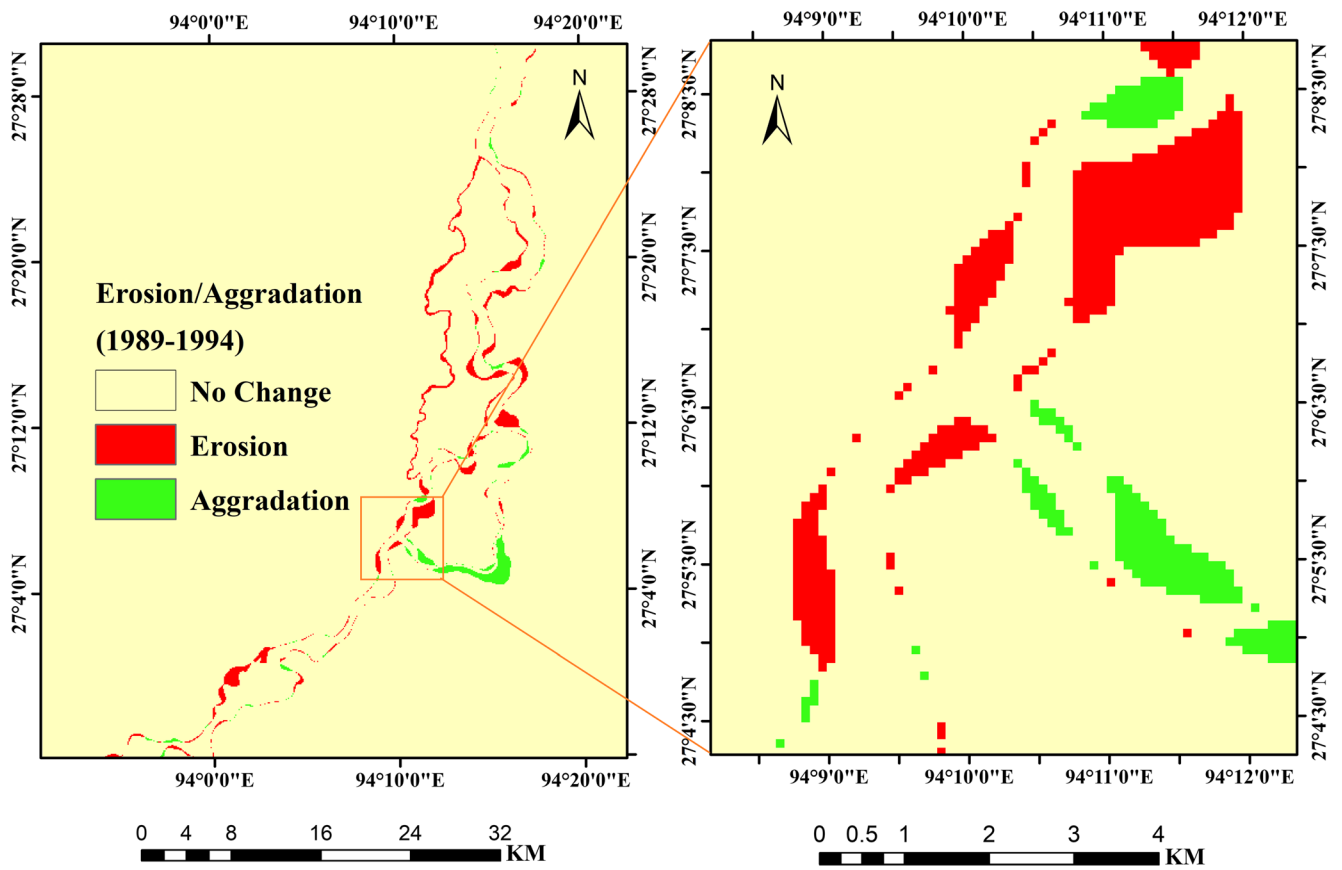


Fig. 10 Map showing erosion and aggradation areas during 1989–1994

Table 3 Transition matrix for 1989–1994

Lateral distance (m)/ d_l	Statistic	Upstream distance (m)/ d_u				
		100	200	300	400–800	800+
100	C	1064	354	139	196	216
	C_e	620	134	49	59	82
	$P_{i,j}$	0.58	0.38	0.35	0.30	0.38
200	C	282	419	291	506	448
	C_e	119	130	64	102	97
	$P_{i,j}$	0.42	0.31	0.22	0.20	0.22
300	C	110	243	254	638	678
	C_e	43	66	51	101	92
	$P_{i,j}$	0.39	0.27	0.20	0.16	0.14
400–800	C	107	385	522	2674	5578
	C_e	35	92	110	261	258
	$P_{i,j}$	0.33	0.24	0.21	0.10	0.05
> 800	C					339,591
	C_e					1396
	$P_{i,j}$					0.00411

Table 4 Flood return periods of the Subansiri River (1988–2017)

Order	Year	Return period (r)	Order	Year	Return period (r)
1	1988	31	3	2003	10.33
2	1989	15.5	8	2004	3.88
6	1990	5.17	10	2005	3.1
12	1991	2.58	11	2006	2.82
5	1992	6.2	9	2007	3.44
17	1993	1.82	7	2008	4.43
16	1994	1.94	22	2009	1.41
18	1995	1.72	23	2010	1.35
19	1996	1.63	25	2011	1.24
13	1997	2.38	24	2012	1.29
15	1998	2.07	26	2013	1.19
21	1999	1.48	27	2014	1.15
20	2000	1.55	28	2015	1.11
14	2001	2.21	30	2016	1.03
4	2002	7.75	29	2017	1.07

Validation of riverbank erosion probability

To validate the applicability of the Eq. 7, the erosion probability for the year 2017 was predicted using the river channel map of the year 2014. The composite distance class map of the year 2014 and flood return interval of 2014–2017 period were used as inputs. The resultant riverbank erosion probability map for the year 2017 was classified into four distinct erosion probability classes/zones: low erosion probability (0–15%), medium erosion probability (15–30%), moderate erosion probability (30–60%), and severe erosion probability (> 60%). The classified erosion probability map of 2017 was then compared with the actual erosion/ aggradation map generated through temporal change detection of river channel maps of 2014 and 2017 (Fig. 11, Table 6).

From Table 6, it is clear that out of total area predicted as high erosion probability zone (> 60% erosion probability), 51.48% area has actually lost to riverbank erosion during 2014–2017. Similarly, 33.93% of area predicted under

Table 5 Flood recurrence interval for the specific time spans

Sl. no.	Time span	Flood recurrence interval ($\sum_{t=1}^n r$)
1	1989–1994	17.7
2	1994–1998	07.8
3	1998–2002	13.0
4	2002–2006	20.1
5	2006–2010	10.6
6	2010–2014	04.9
7	2014–2017	03.2

moderate erosion probability (30–60%) zone actually got eroded due to riverbank shifting from 2014 to 2017. These results obtained by comparing actually eroded area and the erosion probability predicted by the model shows that the model could predict erosion-prone area with an acceptable level of accuracy.

There are a number of factors that influence the riverbank erosion such as height of riverbank, slope of the riverbank, structure and nature of the sediments, land use/land cover of the study area, gradient of the channel, embankments located near the river channel, constraints provided by the bedrocks, mitigation measures taken by government, etc. (Winterbottom and Gilvear 2000). Apart from the distance from the river channel and flood interval, other factors are not taken into consideration in the present study. Despite this limitation of the model, the performance of the model in terms of predicting riverbank erosion is satisfactory. Therefore, the calibrated Graf's model (Eq. 7) developed in this study can be used for quick assessment of riverbank erosion of the Subansiri River in the future that will help in mitigation and management planning. Another important aspect is that the model can be easily implemented in GIS and the required inputs can readily be generated using remote sensing data from various satellite systems which are nowadays available in public domain. It is important to note that the Graf's model is empirical in nature and any change in geographical setting of input data will change the calibration parameters of the model. The performance of the model may further be enhanced by the integration of the most noteworthy elements that put the impetus on riverbank erosion, as stated above.

Conclusions

In the present study, the bank erosion process of the Subansiri River in its highly dynamic and unstable lower 100 km stretch, lying in Assam, India, is studied using geospatial approach. The analysis of temporal remote sensing data for a period of 29 years (1989 to 2017) with time step of 4–5 years indicates that the erosion pattern and rate of erosion vary spatially and temporally. About 103 km² land area got eroded between 1989 and 2017. Identification and analysis of the high riverbank erosion and aggradation zones reveal that, in general, the Subansiri River has shifted towards west, which is in agreement with the observations of earlier researchers. The assessment of riverbank erosion probability using calibrated Graf's model shows satisfactory results. This highlights the potential of the Graf's model in estimating the riverbank erosion probability even in case of a highly dynamic river, considering that it requires limited data inputs and is easily implementable in GIS environment. Since the Graf's model considers only lateral and upstream/downstream distances from the river channel, the inclusion of other factors within the GIS methodology may improve the model performance. We

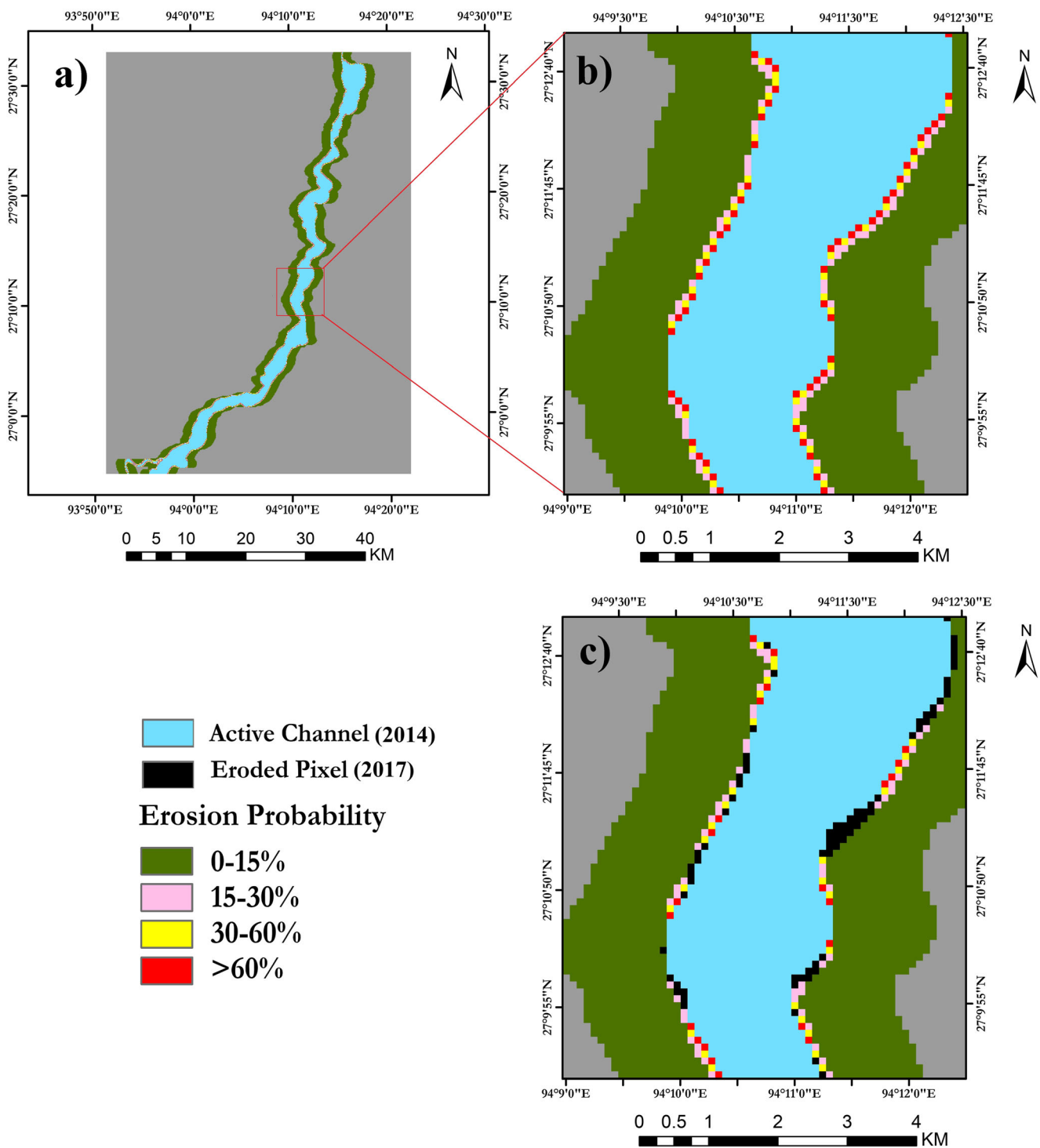


Fig. 11 Erosion probability zones of the year 2014 and actual eroded pixels during time span 2014–2017 overlaid on the probability zone

have used 100 m pixel size for computing the distance classes while implementing the Graf’s model in GIS, mainly to reduce the computation time; however, accuracy and precision may improve if finer pixel size is taken.

The study demonstrates the strength of geospatial approach for rapid assessment of riverbank erosion of alluvial channels.

The understanding developed about the migration behavior of the Subansiri River in the last three decades along with the calibrated Graf’s model for quick assessment of erosion probability in the future will help the concerned authorities to take appropriate mitigation measures and plan river management strategies.

Table 6 Probability zone-wise erosion

Erosion probability zone	No. of land pixels 2014	Eroded land pixels during 2014–2017	Percentage of erosion
0–15%	19,813	844	4.25%
15–30%	1130	276	24.42%
30–60%	554	188	33.93%
> 60%	841	433	51.48%

Acknowledgments This study is part of the Postgraduate Diploma project work carried out by the first author under the IIRS-ITC joint education programme. Thanks to United States Geological Survey for providing Landsat data and to Water Resource Department, Assam, for providing the observed discharge data required for this study. We sincerely thank the Director, Indian Institute of Remote Sensing (IIRS), Indian Space Research Organisation (ISRO), Dehradun, India, for his constant support and encouragement.

References

- Akhter S, Eibek KU, Islam S, Towfiqul Islam ARM, Chu R, Shuanghe S (2019) Predicting spatiotemporal changes of channel morphology in the reach of Teesta River, Bangladesh using GIS and ARIMA modeling. *Quat Int* 513(July 2018):80–94
- Buffington JM (2012) Changes in channel morphology over human time scales. *Processes, Tools, Environments, Gravel-Bed Rivers*, pp 433–463
- Darby SE, Thorne CR (1995) Bank stability algorithm for numerical modeling of channel width adjustment. Report of US Army Research, Development and Standardization Group-UK, London
- Das JD, Dutta T, Saraf AK (2007) Remote sensing and GIS application in change detection of the Barak River channel, N.E. India. *J Indian Soc Remote Sens* 35(4):301–312
- Das TK, Haldar SK, Gupta ID, Sen S (2014) River bank erosion induced human displacement and its consequences. *Living Rev Landsc Res* 8(1):1–35
- Deb M, Ferreira C (2015) Planform channel dynamics and bank migration hazard assessment of a highly sinuous river in the north-eastern zone of Bangladesh. *Environ Earth Sci* 73(10):6613–6623
- Dewan A, Corner R, Saleem A, Rahman MM, Haider MR, Rahman MM, Sarker MH (2017) Assessing channel changes of the Ganges-Padma River system in Bangladesh using Landsat and hydrological data. *Geomorphology* 276(October):257–279
- Dikshit KR, Dikshit JK (2014) North-East India: land, people and economy. Springer Publications, Dordrecht
- Eaton BC, Millar RG, Davidson S (2010) Channel patterns: braided, anabranching, and single-thread. *Geomorphology* 120(3):353–364
- Elliott CM, Huhmann BL, Jacobson, RB (2009) Geomorphic classification of the lower Platte river, Nebraska: U. S. Geological Survey Scientific Investigations Report 2009–5198, 29 p
- Ety NJ, Rashid MS (2019) Spatiotemporal variability of erosion and accretion in Ganges River using GIS and RS: a comparative study overlapping Rennell’s map of 1760s. *Environ Dev Sustain*. <https://doi.org/10.1007/s10668-019-00317-4>
- Florsheim JL, Mount JF, Chin A (2008) Bank erosion as a desirable attribute of rivers. *BioScience* 58(6):519
- Gogoi C, Goswami DC (2013) A study on bank erosion and bank line migration pattern of the Subansiri River in Assam using remote sensing and GIS technology. *Int J Eng Sci* 2(9):01–06
- Gogoi C, Goswami DC (2014) A study on channel migration of the Subansiri river in Assam using remote sensing and GIS technology. *Curr Sci* 106(8):1113–1120
- Goswami U, Sarma JN, Patgiri AD (1999) River channel changes of the Subansiri in Assam, India. *Geomorphology* 30(3):227–244
- Goyal MK, Shivam S, A. K, Singh DS (2018) Subansiri: largest tributary of Brahmaputra River, Northeast India. In: Sen Singh D (ed) *The Indian rivers*. Springer Hydrogeology. Springer, Singapore. https://doi.org/10.1007/978-981-10-2984-4_36
- Graf WL (1984) A probabilistic approach to the spatial assessment of river channel instability. *Water Resour Res* 20(7):953–962
- Heitmuller FT (2014) Channel adjustments to historical disturbances along the lower Brazos and Sabine Rivers, south-central USA. *Geomorphology* 204:382–398
- Khan SS, Islam T (2015) Anthropogenic Impact on Morphology of Teesta River in Northern Bangladesh: An Exploratory Study. *J Geosci Geomatics* 3(3):50–55
- Lanzoni S, Ferdousi A, Tambroni N (2018) River banks and channel axis curvature: effects on the longitudinal dispersion in alluvial rivers. *Adv Water Resour* 113(October 2017):55–72
- Leopold LB, Worman MG, Miller JP (1964) Fluvial processes in geomorphology. W. H. Freeman, San Francisco, Calif
- Leys KF, Werritty A (1999) River channel planform change: software for historical analysis. *Geomorphology* 29(1):107–120
- Lilhare R, Garg V, Nikam BR (2014) Application of GIS coupled modified MMF model to estimate sediment yield on a watershed scale. *J Hydrol Eng ASCE* 20(6):C5014002–C5014001 16
- Midha N, Mathur PK (2014) Channel characteristics and planform dynamics in the Indian Terai, Sharda River. *Environ Manag* 53(1):120–134
- Mount NJ, Tate NJ, Sarker MH, Thorne CR (2013) Evolutionary, multi-scale analysis of river bank line retreat using continuous wavelet transforms: Jamuna River, Bangladesh. *Geomorphology* 183:82–95
- Nanson GC, Knighton DA (1996) Anabranching rivers: their cause, character and classification. *Earth Surf Process Landf* 21(3):217–239
- Nawfee SM, Dewan A, Rashid T (2018) Integrating subsurface stratigraphic records with satellite images to investigate channel change and bar evolution: a case study of the Padma River, Bangladesh. *Environ Earth Sci* 77(3):1–14
- Pati JK, Lal J, Prakash K, Bhusan R (2008) Spatio-temporal shift of western bank of the Ganga river, Allahabad city and its implications. *J Indian Soc Remote Sens* 36(3):289–297
- Rozo MG, Nogueira ACR, Castro CS (2014) Remote sensing-based analysis of the planform changes in the Upper Amazon River over the period 1986–2006. *J S Am Earth Sci* 51:28–44
- Sarkar A, Garg RD, Sharma N (2012) RS-GIS based assessment of river dynamics of Brahmaputra River in India. *J Water Resour Prot* 04(02):63–72
- Singh V, Sharma N, Ojha CSP (eds) (2004) *The Brahmaputra Basin water resources*. Springer Netherlands
- Sinha R, Ghosh S (2012) Understanding dynamics of large rivers aided by satellite remote sensing: A case study from Lower Ganga plains, India. *Geocarto Int* 27(3):207–219
- Sreenu MTL, Teja T (2015) Control of brushless DC motor with direct torque and indirect flux using SVPWM technique. *Indian J Sci Technol* 8(November):507–515
- Subramanya K (2008) *Engineering Hydrology*. In: Mukherjee S (ed) Tata McGraw Hill Publishing Company Limited, New Delhi
- Thakur PK, Laha C, Aggarwal SP (2012) River bank erosion hazard study of river Ganga, upstream of Farakka barrage using remote sensing and GIS. *Nat Hazards* 61(3):967–987
- Tiegs SD, Pohl M (2005) Planform channel dynamics of the lower Colorado River: 1976–2000. *Geomorphology* 69(1–4):14–27
- Winterbottom SJ, Gilvear DJ (2000) A GIS-based approach to mapping probabilities of river bank erosion: Regulated River Tummel, Scotland. *Regul Rivers Res Manag* 16:127–140